CrystEngComm

Reaction Intermediates Induced Vapor-Liquid-Solid Growth of Silicon Oxide Nanowires

Journal:	*CrystEngComm*
Manuscript ID	CE-ART-07-2018-001115.R1
Article Type:	Paper
Date Submitted by the Author:	10-Sep-2018
Complete List of Authors:	Huson, Joseph; University of North Carolina at Charlotte, Department of Mechanical Engineering and Engineering Science Sheng, Tao; University of North Carolina at Charlotte, Department of Physics and Optical Science, and Optical Science and Engineering Program Ogle, Ezekiel ; University of North Carolina at Charlotte, Department of Mechanical Engineering and Engineering Science Zhang, Haitao; University of North Carolina at Charlotte, Department of Mechanical Engineering and Engineering Science

Reaction Intermediates Induced Vapor-Liquid-Solid Growth of Silicon Oxide Nanowires

Joseph J. Huson, [a] *Tao Sheng,* [b] *Ezekiel Ogle,* [a] *and Haitao Zhang* [*a]

ABSTRACT: Vapor-liquid-solid (VLS) process is the most popular vapor-phase method for the controlled growth of various one-dimensional (1D) nanostructures with the assistance of catalyst particles. In a typical VLS process, precursors for the desired deposition are introduced intentionally during the growth and catalysts are employed to promote the formation of 1D nanostructures. However, in this study, we report a new VLS growth mode for unexpected 1D nanostructure growth without directly introducing corresponding source materials. In the nanostructure growth of a compound semiconductor, ZnTe, besides the expected ZnTe nanowire arrays, unexpected growth of "jellyfish-like" SiO_x nanowires has been observed. The study of growth mechanism reveals that the reaction intermediates from the ZnTe growth, Te-based vapor species, induced the growth by producing Si vapor, while Au catalysts promoted the growth of the nanostructures. Detailed growth processes in this new VLS mode have been analyzed. This study will promote the attentions in composition and phase controls for the growth of compound semiconductor nanostructures. The new growth mode can be extended to realize convenient growth of other nanomaterials with lower temperature and low cost.

1 Introduction

During the extensive development of nanotechnology in recent decades, intensive research efforts have been focused on one-dimensional (1D) nanostructures in pursuit of their great potentials in fabricating miniature devices with better performance, lower manufacturing cost, and lesser power consumption.[1] Among various vapor-based synthesis methods, vapor-liquid-solid (VLS) growth mechanism has been the most successful and versatile strategy for the controlled growth of various 1D nanostructures with the assistance of catalyst particles.[1-2] In a conventional VLS process, source materials for desired deposition must be first introduced into the reaction chamber in forms of different types of precursors (*i.e.*, solid, liquid, or gas phases). In the growth zone, the catalyst particles accommodate vapor reactants from the source forming liquid droplets. The droplets reach to supersaturation, followed by the nucleation and growth of 1D nanostructures. Therefore, the catalyst particles will promote and guide the 1D growth with advantages of fine controls of location, orientation, dimension, and morphology of the nanostructures.[2-3]

In the study of VLS growth, most attention has been focused on the effects of catalysts in promoting, guiding, and controlling the growth of 1D nanostructures. A variety of catalysts have been extensively employed and studied, including noble and transitional metals (*e.g.*, Au, Pt, Ti, and Fe, *etc.*),[4] low melting temperature metals (*e.g.*, Ga, In and Sn, *etc.*),[5] non-metal elements (like Ge)[6], and even compound materials (*e.g.*, Ag_2Se, Cu_2S, and alkali metal based compounds, *etc*.).[7] However, from the source materials to the final depositions, there are many possible chemical reations producing a variety of reaction intermediates. The roles of these intermediates in the nanostructure growth have been normally ignored without attracting much research efforts. Here, we report a new VLS growth mode induced by the reaction intermdiates. In the VLS

growth of Zinc Telluride (ZnTe) nanowires using gold (Au) catalysts, unexpected growth of "jellyfish-like" SiO_x nanowires has been found among the desired deposition of ZnTe nanowire arrays, while no Si source materials were directly used. Mechanism study has been performed to reveal the growth mechanism of these jellyfish-like nanowires. It is found that the Te-based reaction intermediates from the ZnTe source play an important role in inducing the SiO_x 1D nanostructures. Different from the normal catalysts used in a conventional VLS growth, these Te-based intermediates do not directly promote the growth nanowires. They induce the SiO_x growth by producing Si vapor for the growth, while Au serves as classic catalysts promoting the nanostructure growth. This result is of essential importance for the future development of 1D nanostructures. The effects of the intermediates in the growth of 1D compound nanostructures cannot be ignored, as they may introduce different compositions and even different phases into the final deposition. On the other hand, the similar growth mechanism can be extended to other materials to facilitate nanostructure growth at lower growth temperature and lower cost.

2 Experimental

2.1 Materials synthesis system

The experiments were performed using a home-built hot-wall low-pressure chemical vapor deposition (CVD) system based on resistance heating. The system is similar to the CVD system employed in previous reports,[7b, 8] with modifications of an automatic pressure regulating system (MKS Instruments) composed of a throttle control valve (MKS 653B), a pressure controller (MKS 600), and a MKS capacitance manometer (Baratron). The process pressure can be maintained from several mTorr to hundreds of Torr.

2.2 Substrate preparation

Silicon (100) substrates (p-type, University Wafers) were used in the experiments. The substrates were first cut into ~ 10 mm × 40 mm pieces and ultrasonically cleaned with acetone and ethanol for 15 minutes each, followed by blow-drying with nitrogen gas. For catalyst-assisted experiments, the substrates were coated with a ~10 nm of Au layer using a magnetron sputter (Desk IV TSC, Denton Vacuum) prior to the growth. Au coated Si substrates were employed in all the experiments for the ZnTe growth and the SiO_x growth. Bare Si substrates without Au coating were used in some control experiments for the growth mechanism study, which will be specified in the context.

2.3 Growth process

For the growth of zinc telluride (ZnTe) nanostructures, ZnTe powders (Alfa Aesar, 99.99%) were used as the source materials. In a typical synthesis, ZnTe powders were loaded at the center of the reaction chamber with the receiving substrate located 2" downstream of the source. After loading the source and substrate, the reaction chamber was first pumped down to an ultimate vacuum pressure ~5 mTorr. 30 sccm (standard cubic centimeter per minute) of UHP (ultra-high purity) Argon (Ar) and 1.5 sccm of UHP hydrogen (H_2) were then introduced into the chamber. Typical pressure employed for the growth was 50 Torr, controlled by the automatic pressure control system. Other growth pressures were also explored within the range of ~ 20 Torr - 200 Torr. The furnace was then heated to 850 °C in 30 min, and held for 60 min, followed by cooling down to room temperature in a few hours. The heating temperature across the substrate was determined to be ~ 812 °C - 565 °C (from upstream end to downstream end) according to the temperature profile of the furnace measured at atmospheric pressure.

For control experiments and growth mechanism study, tellurium (Te, Sigma-Aldrich, 99.8%) and zinc (Zn, Alfa Aesar, 99.9%) powders were used independently to determine their effects on

the formation of SiO_x nanowires. During the control experiments, the Te or Zn powders were placed at different locations at upstream of the furnace to adjust its vapor pressure. All reactants were used as received without further processing. After the cooling, the substrates and source powders were then taken out for characterization.

2.4 Materials Characterization

The as-synthesized samples were analyzed using scanning electron microscopy (SEM, JEOL JSM-6480 and Raith 200), energy dispersive X-ray spectroscopy (EDS, Oxford Instrument INCA), X-ray diffraction (XRD, PANalytical X'pert Pro MRD with Cu Kα radiation at λ = 1.5418 Å), and transmission electron microscopy (TEM, JEOL JEM-2100 LaB_6 operated at 200 kV).

3 Results and discussion

Typical ZnTe deposition on an Au coated Si substrate is shown in Fig. 1. Figure 1a shows its overall morphological changes along the substrate that are visible to the naked eyes. The dense deposition exhibits a bright red color, same as the ZnTe powders used for growth. Four distinct growth zones can be identified with growth temperature changes from high to low. At high growth temperature (~812 °C – 769 °C), large islands grown on the substrate are shown in Fig. 1b. Ultra-long microwires (Fig. 1c) are found in a growth zone ranging from ~ 769 °C to 727 °C. The microwires can grow into a few centimeters in length, which is just limited by the growth time and the dimension of the reaction chamber. A close-up (inset of Fig. 1c) shows the surface facets of the microwires indicating twin formation as reported previously.[9] From ~ 727 °C to 687 °C is the growth zone of straight nanowires (Fig. 1d), which are hundred nanometers in diameter with length up to several millimeters. Figure 1e shows thinner nanowires (Fig. 1e) with branches

at the tips of nanowires (inset of Fig. 1e) in the growth zone from 687 °C to 641 °C. The side-view of the branched nanowire zone (Fig. 1f) shows it has a two-tier structure: some nanowires that grew much taller (mm scale) have branches at their tips forming the canopy on the top (Fig. 1g), while thin nanowires at the bottom (hundred microns in length) have no branched tips (Fig. 1h). This two-tier structure indicates that there was a growth competition among the dense nanowires. The nanowires initially taller would grow faster as they were exposed openly to the source vapors forming the top layer. On the other hand, those shorter ones would grow slower forming the bottom layer, due to the difficulty to reach the source vapors as the nanowires grew denser. The branched structures only appearing at the tips of the long nanowires shows they formed by the end of the growth. It is most probably during the cooling step, as the lower growth temperature would promote the condensation at the tips of the nanowires forming the branched structures.

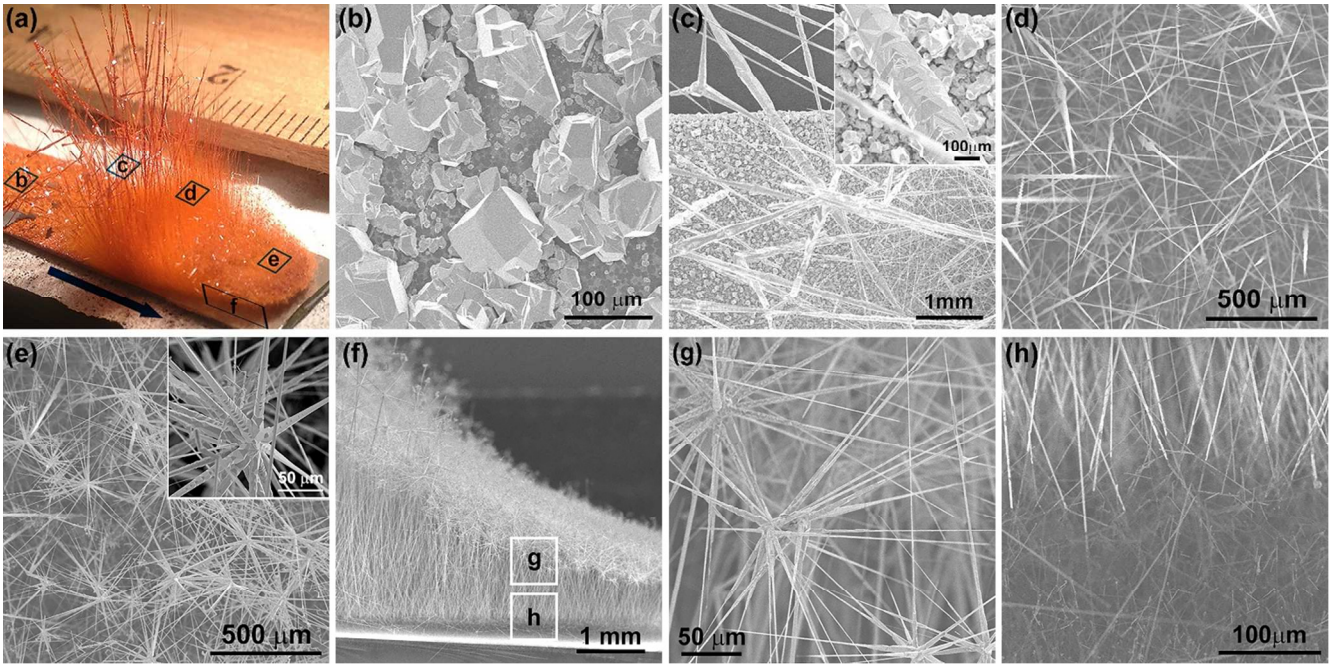

Figure 1. CVD growth of ZnTe nanostructures. (a) Photo of ZnTe deposition overview on substrate showing morphological changes of different growth zones as the growth temperature

decreases along the flow direction (indicated by the arrow). (b-e) Top-view SEM images of ZnTe growth zones at different locations as labeled in (a): (b) islands, (c) ultra-long microwires with the inset of high-magnification image showing surface facets, (d) straight nanowires, and (e) branched nanowires with the inset of the branched tips. (f-g) Side-view (f) low magnification SEM image of the branched nanowires and (g-h) high magnification images showing the (g) top layer and (h) bottom layer.

The composition of the deposition was determined using EDS in SEM. Figure 2 shows typical results from the stem of microwires (Fig. 2a) and the tip of branched nanowires (Fig. 2b). From the microwires, EDS spectrum (Fig. 2c, bottom spectrum) show strong Te and Zn peaks with negligible O signal probably due to slight surface oxidation. The ratio of atomic percentages between the Zn and Te is 50.96:49.04 ≈ 1.04:1, very close to the 1:1 stoichiometry of ZnTe. However, at the tip of the branched nanowires (Fig. 2c, top spectrum), a strong Si peak is found besides the Zn and Te signals. Careful examination was performed on multiple locations of the branched nanowires. The strong Si signal only showed up at the tips, while no Si signal was found from the stems of the nanowires. The Si peak at the tips of branched ZnTe nanowires is not from the background Si substrate and its origin will be discussed later in the context. The crystallinity of the deposition was confirmed by XRD (Fig. 2d), with diffraction peaks match closely the standard pattern of the cubic zincblende ZnTe phase (ICDD PDF # 00-015-0746, a = 6.1026 Å). The growth of ZnTe micro- and nanostructures is similar to the previous report.[9] The growth mechanism is dominated by the VLS growth with Au particles as the catalysts promoting the axial growth, while the vapor-solid growth accounts for the radial growth resulting in the thick diameter of the microwires and the tapered growth of nanowires.[9] ZnTe growths at different growth pressures from 20 Torr to 200 Torr were explored. The growth yield of ZnTe

reached its highest at the growth pressure of ~ 50 Torr, and it became lower when the growth pressure was away from 50 Torr. More interesting, un-expected jellyfish-like nanostructures (Fig. 2e-h) were found among the ZnTe deposition when the ZnTe yield was low. These nanostructures appeared among the ZnTe deposition with a low density. Their growth locations varied randomly across the whole substrate in different experiments, i.e., in a growth they could appear at some zones among the growth zones b-e shown in Fig.1. Despite of the detailed differences in morphology, these nanostructures all have large particles on top of tentacles-like tiny nanowires with diameters of a few nanometers and lengths up to tens of microns. It is important to figure out what materials these nanostructures are and how they formed during the ZnTe growth. Therefore, the focus of this report is centered on exploring the growth mechanism of this unexpected growth of nanostructures and revealing the detailed atomic processes during the nanostructure formation.

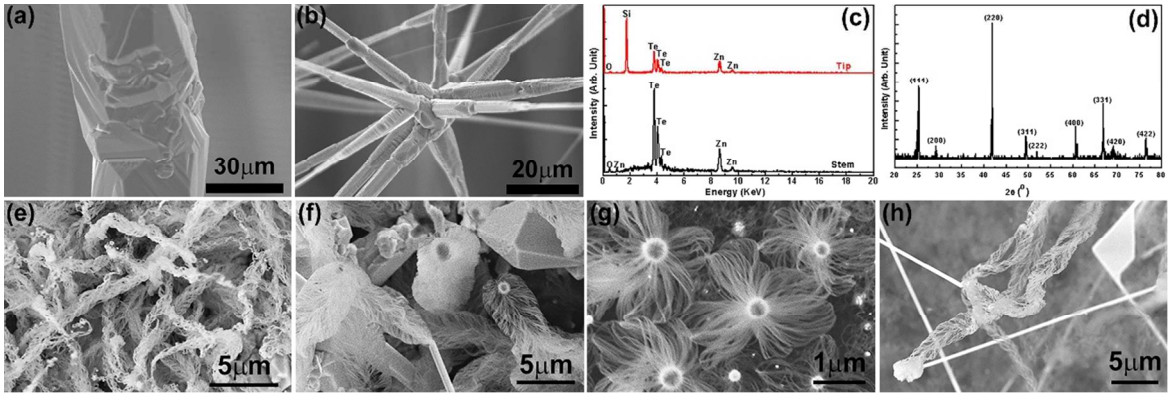

Figure 2. (a-b) SEM images of (a) stem of a ZnTe microwire and (b) tip of a branched nanowire, (c) corresponding EDS spectra for (a) and (b), and (d) XRD spectrum of ZnTe deposition. (e-h) SEM images of different jellyfish-like nanostructures.

A series of control experiments have been performed to investigate the growth mechanism of these jellyfish-like nanostructures. One experiment was carried out without any source materials. Only an Au coated Si substrate was loaded with all other growth parameters kept same as those for the typical ZnTe growth. Shown in Fig. 3a, no nanostructures were found except gold

nanoparticles on the substrate surface. The gold nanoparticles formed due to the thermal annealing of the Au coating during the growth. This result rules out the possibility that these nanostructures could be induced by Au catalyst alone on the substrate under the growth conditions employed in this study. Therefore, the growth of the jellyfish-like nanostructures must relate to the by-products from the ZnTe source. During the ZnTe growth, ZnTe source could sublimate and react with H_2, producing a variety of reaction intermediates in the vapor phase including ZnTe, Zn, Te, Te_2 and H_2Te, etc.[10] First, the role of Zn vapor was identified by an experiment using Zn powders as the source materials. The Zn powders was located upstream at ~ 300°C producing a vapor pressure ~ 1.45mTorr.[11] As shown in Fig. 3b, only tiny Au particles were found on the substrate showing Zn vapor could not induce the nanostructure growth. The resulting Au particles are smaller than those particles in Fig. 3a probably due to the dissolution of Zn into the Au.

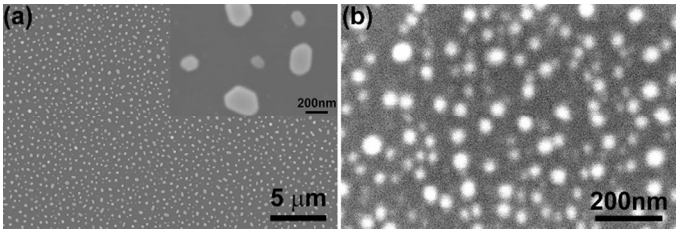

Figure 3. SEM images of the substrates after (a) the growth without any source material and (b) the growth using Zn powders as source material. Both growths show only Au particles on the surface.

Next, Te powders were used as the source material to verify the effects of Te-based species in the nanostructure growth. The Te powders were located upstream at ~ 670 °C with a vapor pressure of ~ 16.7 Torr.[12] Nanostructures with different morphologies were found on the substrate as shown in Fig. 4. High density of jellyfish-like nanostructures were found in a growth zone with the growth temperature from ~758 °C (Fig. 4a) to ~ 624 °C (Fig. 4b). Beyond this

growth zone with higher growth temperature upstream (~ 812 °C – 758 °C), the nanostructures quickly become shorter and disappear. At downstream locations, along the substrate the deposition gradually morphs into thick nanowires at ~ 612 °C (Fig. 4c), short nanorods at ~ 600 °C (Fig. 4d), and nanospheres at ~565 °C (Fig. 4e). All the jellyfish-like nanostructures have ball-shaped catalyst particles on top of dense and long nanowire tentacles. On the other hand, most of the thick nanowires in Fig. 4c have a structure with single nanowire beneath each catalyst particle. This morphology change can be attributed to the lower growth temperature that promotes the bundling and merging of thin nanowire tentacles forming one thick nanowire. The formation of nanorods and nanospheres downstream is due to the further decrease of growth temperature and the reduction of vapor supplies. The nanorods have a mushroom-like structure with a large catalyst top above a short and thick stem, while the nanospheres exhibit a core-shell structure with deposition wrapping outside the catalyst particle. EDS analyses (Fig. 4f) were performed at different locations. All the nanostructures have large signals from Si and O indicating the deposition of SiO_x, while the Au signals are from Au catalysts. It is worth mentioning that no Te signals are found for all the nanowires (Fig. 4f, top curve), both the jellyfish-like and the thick ones, while Te signals are clearly present in the nanorods (Fig. 4f, middle) and nanospheres (Fig. 4f, bottom) regions. This result indicates that the Te content is lower than the detection limit of EDS in the nanowires grown at high temperature (above ~ 612 °C), while more Te content is able to form in nanorods and nanospheres due to their lower growth temperature (~ 600-565 °C).

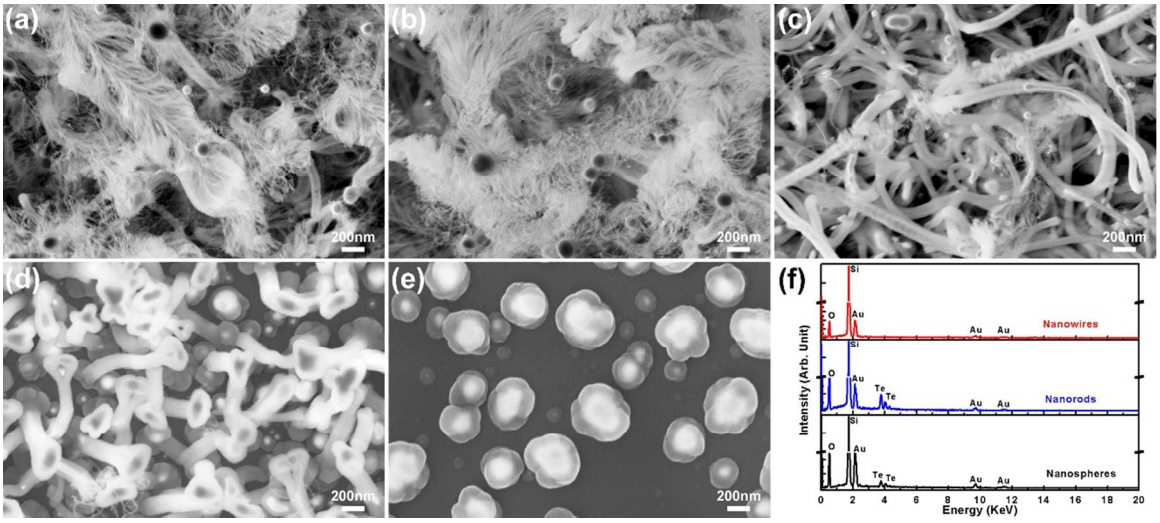

Figure 4. (a-e) SEM images of SiO_x nanostructures at different growth temperatures: (a-b) jellyfish-like thin nanowires, (c) thick nanowires, (d) mushroom-like nanorods, and (e) core-shell nanospheres. (f) Corresponding EDS spectra of the deposition with different morphologies.

Since the Si and O signals could also come from the background of the Si substrate, TEM analyses were performed on the nanostructures to further confirm their composition and identify their structures. Study has been mainly focused on the jellyfish-like nanowires and the results are shown in Figure 5. Figure 5a shows a typical jellyfish-like nanostructure with lots of nanowire tentacles attached to one large catalyst particle. Figure 5b show a nanostructure with only one straight nanowire attached to the particle, but it is also possible that other nanowire tentacles were lost during the sample transferring from the substrate to the TEM grid. Figure 5c shows a similar jellyfish-like nanostructure, but the nanowire tentacles have a nodular morphology. All the tentacle nanowires are very thin only a few nm in diameter, while the catalyst particles are larger about 100-200 nm in diameter. The insets in Fig. 5a-b show the catalyst-nanowire interfaces and some branched structures between nanowires. It should be emphasized that the jellyfish-like nanostructures have a significant different catalyst-nanowire interface from the one for the classic VLS growth. For a conventional VLS growth, there is a sharp and straight

interface between the catalyst and the nanowire. However, for the jellyfish-like nanostructures, the whole catalyst particle is wrapped with a thin layer of deposition and the tentacle nanowires are grown on this shell layer of deposition. From the EDS analyses (Fig. 5d), the nanowires can be identified as SiO_x nanowires with strong signal of Si and O, while the catalyst particle is Au alloyed with Si with a thin shell of SiO_x. (Please note the additional Cu, Cr, and C signals were background signals from the TEM column and the sample grid). Again, no Te signals were detected in these jellyfish-like nanostructures, either from the nanowires or from the catalyst particles.

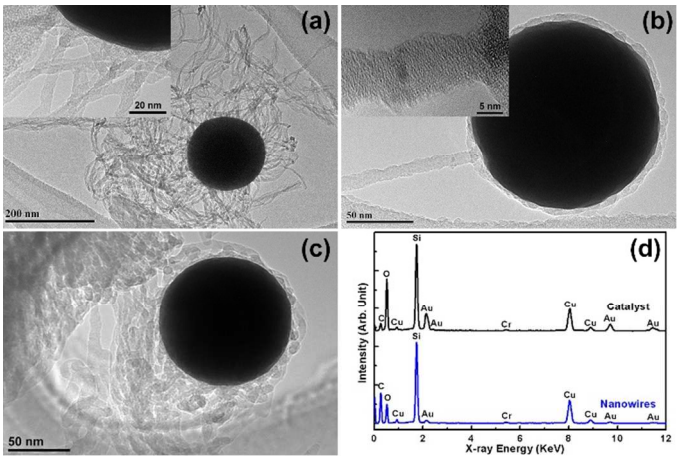

Figure 5. (a-c) TEM images of typical jellyfish-like SiOx nanowires with insets showing structures at the nanowire-catalyst interface, and (d) EDS spectra from the catalyst (top) and nanowires (bottom).

Questions arise based on the above analyses. Why it requires Te source to induce the growth of jellyfish-like nanostructures while no Te was detected in the nanostructures? What is the role of Te in the nanostructure growth? And what are the differences between the functions of Te and Au in the nanostructure growth? To answer these questions and to reveal the growth mechanism of the nanostructures, growth processes have been analyzed in details. First, from the SEM and TEM analyses, it is easy to identify that the Au particles on top of the nanowires serve as the

catalysts promoting the nanowire growth, similar to the conventional VLS growth. A growth was performed using Te source without the Au coating on the substrate, and no deposition was found on the substrate. This result further verifies the function of Au as the catalysts for the VLS growth of the nanostructures. Au is a common catalyst for the VLS growth of Si nanostructures, as the Au-Si system forms eutectic at 363 ± 3 °C with the eutectic composition of 18.6 ± 0.5 at% Si.[13] Si vapor dissolves into the Au forming eutectic liquid droplets. When the Si content reaches beyond its solubility limit in Au, it will precipitate inducing the nanostructure growth.

Therefore, it is essential to answer how the Si vapor was produced during the growth as no Si precursor was introduced into the CVD system except the Si substrate. Considering the experiment facts that the SiO_x nanostructures could not be produced without ZnTe or Te sources, we propose a hypothesis that Te-based vapors can react with solid Si and produce Si vapor for the nanostructure growth. The Si-Te phase diagram shows Te can react with Si forming a compound of Si_2Te_3, which then forms eutectic with Te (i.e., L Φ Si_2Te_3 + Te) at 406 °C with composition of 82.5 at% Te (i.e., 17.5 at% Si).[14] Hence, it is possible that Te can induce Si vapor during the growth assisting the formation of SiO_x nanostructures. To prove this theory, experiments were carried out with Te source heated at 850 °C, where the Te vapor pressure can reach to ~ 2×10^2 Torr (Note: This is the saturated pressure at equilibrium. The total growth pressure was still maintained at 50 Torr with vacuum pumping.).[12] As shown in Fig. 6a, large bubble-like particles formed on the Si substrate surface due to the large amount of Te vapors produced at the high heating temperature. The particles etched deeply into the Si substrate and they could form on either bare Si substrate (Fig. 6b) or Au coated Si substrate (Fig. 6c). These results prove that Te vapors can react with Si substrate forming eutectic particles on the substrate. Corresponding EDS results in Fig. 6d confirm that the composition of the particles are

mainly Si and Te, with O from oxidation and Au for Au coated substrate. All the bubble-like particles have a similar morphology with empty cores and most of them have a wrinkled surface morphology. The bubble-like morphology indicates the eutectic droplets are not stable during the growth. The Te content will be re-evaporated, therefore release Si vapor. This phenomenon produces particles like bubbles blown up by the vapors. After the growth completes and the system is cooled down, some bubbles shrink forming the wrinkled surfaces and some bubbles keep their round shapes probably due to their higher thickness. This analysis also explains why Te signals were not found in all the bubble-like particles in the EDS measurement. Some bubble-like particles have no significant Te signals due to the depletion of the Te content during the growth. Figures 6e-f show an EDS elemental mapping of these Si-Te eutectic particles on an Au coated Si substrate. The mapping shows the Si signal is from everywhere of the substrate (Fig. 6f) but its intensity becomes lower at the locations of these bubble-like particles, while the Te signal (Fig. 6g) is only from these bubble-like particles. This result confirms the bubble-like particles were formed from the Te vapor that reacted with the Si substrate, and the low intensity of the Te signal indicating the consumption of Te during the growth. Due to the thin thickness (10 nm) of the Au coating on the substrate, the Au signal for mapping in Fig. 6h is very low, mostly from the background noises. The EDS mapping of the particles on a bare Si substrate (not shown) was also performed, which is similar to the result showing in Fig. 6f-g just without the Au signal.

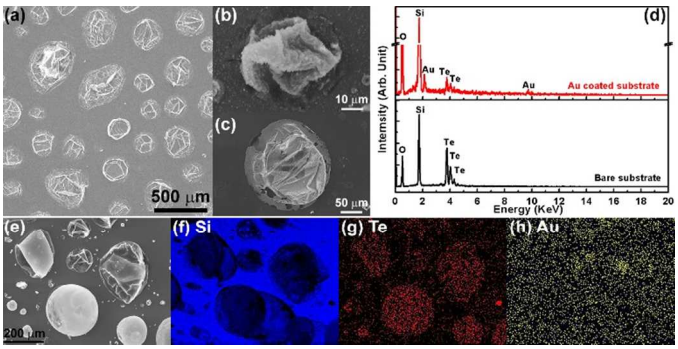

Figure 6. SEM images of (a) Si-Te eutectic particles formed on Si substrate and (b-c) individual particles on (b) Au coated Si and (c) bare Si substrate. Corresponding EDS spectra of (d) the Si-Te eutectic particles. Elemental mapping of (e-f) the Si-Te eutectic particles with (e) SEM image and corresponding EDS signals from (f) Si, (g) Te, and (h) Au, respectively.

Now, the different roles of Te and Au in the SiO_x nanostructure growth are clear. As they both can form eutectics with Si, Te will induce the production of Si-based vapor, while Au will promote the SiO_x nanostructure growth through VLS mechanism. The stability theory of catalysts can successfully explain why Au and Te behave differently in the growth of SiO_x nanostructures. Au has very low vapor pressure at even elevated temperatures, for example, the Au vapor pressure is about 1.09×10^{-5} Torr at its melting temperature T_m= 1046 °C.[15] Therefore, Au catalysts are very stable at the substrate heating temperature (~ 812 °C - 565 °C) with negligible vapor pressure. As a result, Au can serve as catalysts promoting the nanostructure growth, but it cannot produce the Si precursor for the growth at the given experiment condition. On the contrary, Te catalysts are not stable with a low melting temperature at 450 °C. The vapor pressure of Te at 615°C already reaches 7.5 Torr, much higher than the one for Au.[12] This fact explains why there were no Te signals in SiO_x nanowires grown above ~ 612 °C, while small amount of Te was found in nanorods and nanospheres at ~ 600-565 °C. Because of its high vapor pressure, the Te vapors produced from source materials react with Si substrate at high

temperature zone forming eutectic particles, which are subsequently re-evaporated releasing Si vapor for the growth of SiO_x nanostructures at lower temperature zones. Therefore, during the ZnTe growth the Si source was induced by the intermediate Te species, such as Te, Te_2, and H_2Te, etc. The Si contents in the deposition are affected by the dynamics of different reactions during the growth. In the typical ZnTe growth at 50Torr with high yield of ZnTe nanostructures shown in Fig. 1, the Zn species and Te species were balanced. The reaction between Te vapors with Si substrate was negligible, as the ZnTe formation from Zn and Te species was dominant. This analysis explains why Si content was not found in the majority of ZnTe deposition in our growth and previous report.[9] However, Si signals did present at the tips of the branched ZnTe nanowires. The results can be attributed to the changes in reaction dynamics during the cooling stage. As the heating temperature decreased, the balance between the Zn and Te species shifted and promoted the Te-Si reactions to produce Si vapor. The Si vapor was accommodated into the deposition at the tips of the ZnTe nanowires at low growth temperature and this was possible a reason for the formation of the branched nanostructures. When growth conditions changed with growth pressures different from 50 Torr, growth dynamics could change a lot resulting in enhanced Te-Si reactions during the growth stage. This change explains the lower yield of ZnTe deposition and the appearance of more SiO_x nanostructures. Y. L. Chao *et al.* reported the growth of ZnTe-SiO_x core-shell nanostructures using slightly different growth conditions.[10a] They concluded that it was the Au on the first Si substrate at high temperature of 1040 °C that responsible to the evaporation of Si substrate forming the SiO_x shells. However, our results indicate the role of intermediate Te species may not be ignored in the production of Si vapor. Although no SiO_x shells formed without the Au coating on the Si source substrate in their control experiment, it might be due to the high heating temperature of 1040 °C for the Si source

substrate at the center of the furnace. The chance was low for Te vapors to adsorb onto Si substrate and react at such high heating temperature, but the presence of Au could possible incorporate the Te species forming Au-Te-Si eutectic and producing Si through re-evaporation. Additional experiments without the ZnTe source may help to clarify the details.

Based on all the experiment results and the mechanism analyses, we propose the growth mechanism of the SiO_x nanostructures with detailed atomic processes as demonstrated in Fig. 7. In the source zone (Fig. 7a), the ZnTe source sublimates and reacts with H_2 producing various Te-based intermediates (e.g., Te, Te_2, and H_2Te etc.). Similar processes occur if the source is replaced by the Te powders. The Te-based vapors are transferred downstream. They will first interact with the Si substrate at high temperature end (~ 812 °C – 758 °C), i.e., the Si-vapor production zone (Fig. 7b). The Te species react with Si on the surface forming eutectic particles, which may also contain Au from the Au coating on the substrate (Fig. 7b-I). Due to the instability of the Te-Si eutectic particles, the particles evaporate and release Te and Si vapor into the reaction chamber (Fig. 7b-II). The Si vapor induced by the Te species become the source for the SiO_x nanostructure formation on the substrate at lower temperature end, i.e., the nanostructure growth zone (Fig. 7c). SiO_x nanostructures form on the substrate with different morphologies, including jellyfish-like nanowires (Fig. 7c-II), thick nanowires (Fig. 7c-III), nanorods (Fig. 7c-IV), and nanospheres (Fig. 7c-V). The nanostructure formation follows the VLS mechanism. The formation of SiO_x might be due to the residue O_2 in the reaction chamber. However, the resulting nanostructures were most probably amorphous Si under the reduction growth condition provided by the H_2 flow. The amorphous Si nanostructures were subsequently oxidized into SiO_x when they were exposed to the air after the growth. As different from the conventional VLS nanostructures, the formation of jellyfish-like nanowires is discussed here in

details. The evolution of the jellyfish-like nanowires with growth time is schematically demonstrated in Fig. 7c-I. The nanostructure growth is promoted by the Au catalysts, which form eutectic particles with Si vapor in the growth zone. The round-shaped particles indicate the catalysts are liquid droplets during the growth. In a classic VLS growth, after the catalysts are saturated with source materials, deposition precipitates out of the catalysts forming a sharp straight liquid-solid interface. This liquid-solid interface will then serve as the growth front guiding the growth of nanowires. However, as revealed by the TEM results (Fig.5), in our experiments Si will precipitate all over the surface of the saturated Au catalysts forming shells of amorphous Si outside the catalysts. During the growth, the continuous supply of Si will diffuse along the surface of the amorphous Si shells, nucleate and form first a few nanowires. As the nanowires growth longer, the core-shell catalysts are lifted up. More nucleation can happen on the surface of the Si shells forming more nanowires. The multiple nucleation sites on the surface of the Si shells result in the jellyfish-like nanostructures with many nanowire tentacles. The nanowire nucleation could also occur on the surface of existing nanowires forming branched nanowires. Nanowires can curve during the growth producing twisted nanostructures. Schematic drawings of these typical nanowires are demonstrated in Fig. 7c-II. It is worth noting that in the conventional VLS growth, each catalyst particle can only induces one nanowire dictating the shape and dimension of the nanowire. For the growth of the jellyfish-like nanostructures in this report, one large catalyst particle induces the growth of many nanowires. Therefore, the shape and dimension of these nanowires are not controlled by the dimension of the catalyst particles. They are most probably controlled by the dimension of the nucleation sites on the Si shells of the catalysts. With the decrease of the growth temperature downstream, surface diffusion of Si decreases promoting faster nucleation. Together with the reduced Si-based vapor supply to

downstream, the nanostructures grow thicker and shorter producing thick nanowires, nanorods, and nanospheres (Fig. 7c-III-V).

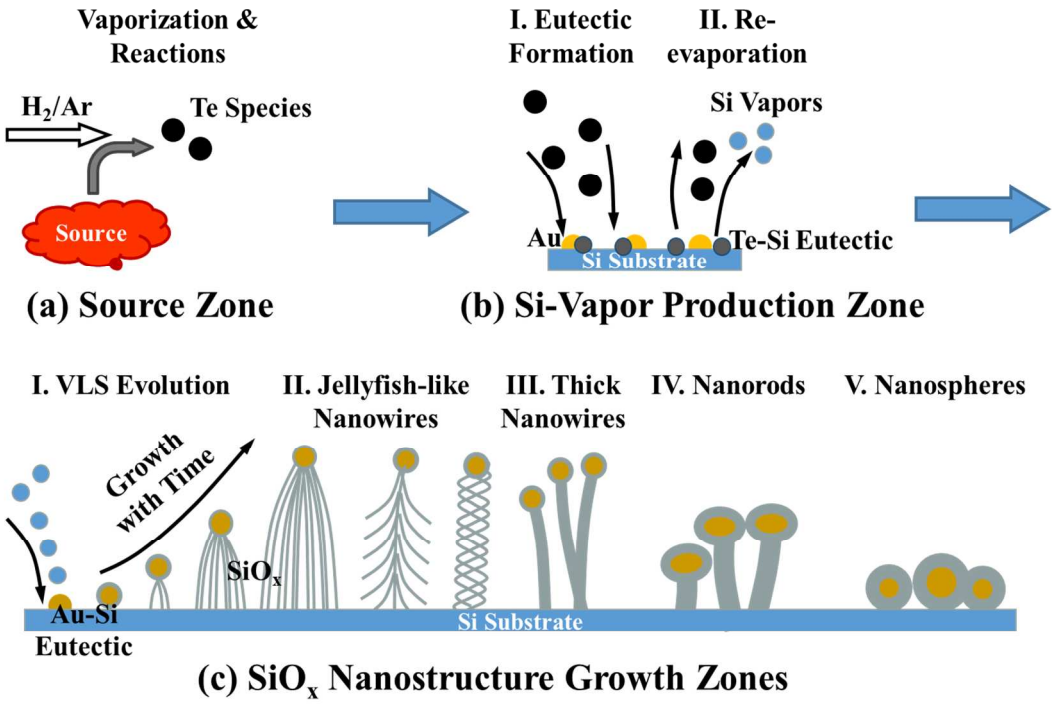

Figure 7. Schematics of growth mechanism and physical processes of the SiO_x nanostructures: (a) source zone produces Te-based species, (b) Si-vapor production zone on Si substrate at high temperature end, and (c) growth zones of SiO_x nanostructures on Si substrate at lower substrate temperature.

As discussed above, the Si vapor was not supplied intentionally for the growth of SiO_x nanostructures in our experiments. It was induced by the reaction intermediates of Te-based species. Therefore, it deserves to make a comparison to other reports of SiO_x nanostructures with similar morphologies. This comparison will help us to have a better understanding of the growth mechanism and atomic processes during the growth. Table 1 listed some typical reports on the growth of SiO_x nanostructures with close morphologies. The majority of the previous reports have employed Si precursors to produce Si-based vapors and catalysts to promote the

nanostructure growth. Z. W. Pan *et al.* first reported the growth of similar amorphous SiO_x nanostructures induced by the Ga droplets from GaN decomposition.[5b] The Ga droplets served two roles in their report: (1) producing Si vapor by etching the Si substrate and the releasing Si at high temperature and (2) promoting the SiO_x growth as catalysts at low temperature. In their later report, the Si source was replaced by SiH_4 without the need of assistance of the Ga droplets.[16] Many groups employed SiO as the Si source for the growth by evaporating of SiO powders or by oxidizing and evaporating Si in residue O_2 environment.[17] Mechanism investigations have shown that the volatile SiO species produced from high temperature annealing of Si with low residual O_2 contents are the essential precursors for the growth of SiO_x nanostructures.[18] Some claimed direct evaporation of Si substrate or powders to produce Si vapor for the growth,[19] however, the formation and evaporation of SiO could not be ruled out due to the presence of the residue O_2. In these reports, residue O_2 or air leakage were responsible for the formation of SiO_x and different types of metal catalysts were used to promote the growth of the SiO_x nanostructures. In this work, the formation of SiO_x nanostructures was discovered among the ZnTe growth without intentionally introducing the Si source. Two elements played different roles important to the SiO_x growth: the intermediate Te-based species from the ZnTe induced the Si source by dissolving the Si substrate and releasing Si vapor, while Au served as the catalysts to promote the nanostructure growth. Therefore, this phenomenon is important for the composition and phase controls in the growth of compound nanostructures in which by-products may be induced by reaction intermediates. Based on the growth mechanism unveiled, experiments were modified to a high-yield growth of SiO_x nanostructures by using Te powders as the source materials. Compared to other reports, this result provides a convenient and low-cost method with much lower heating and growth temperatures as summarized in Table 1. This work can be further

developed to become "greener" and more cost-efficient. For example, using Te as a transport agent, Si vapor can be produced directly from low-cost Si powders for the growth of different Si-based nanostructures without using those expensive and hazardous precursors (*e.g.*, SiH_4). Other elements that can form eutectics with Si and subsequently evaporate to release the Si vapor could also be searched. Inexpensive catalysts, such as Cu, are possible to be employed to replace expensive Au to promote the nanostructure growth. Crystalline nanostructures could also be produced by adjusting the growth temperature and other growth parameters.

Table 1. Comparison between similar growths of SiO_x nanostructures.

References	**Si Source**	**VLS Catalysts**	**Heating Temperature**	**Growth Temperature**
Z. W. Pan *et al.*, 2002[5b]	Si etching and releasing by Ga (from GaN decomposition)	Ga from GaN decomposition	1150 °C	1000 – 850 °C
Z. W. Pan *et al.*, 2003[16]	SiH_4	Ga from GaN decomposition	1150 °C	1100 °C – 950 °C
C. L. Pang *et al.*, 2011[17a]	SiO powders	Ge powders	1600 °C	1600 °C
M. N. Banis *et al.*, 2011[17b]	SiO from Si + residue O_2	VO_2 and Au	1000 °C	1000 °C
J. Y. Qu et al., 2012 [17c]	SiO from Si + residue O_2 and/or $SiCl_x$ from Si + HCl	Fe from $FeCl_3$ + H_2	1000 – 1200 °C	1000 – 1200 °C
R. G. Elliman *et al.*, 2012[17d]	SiO from Si + O_2 impurity (enhanced by Au)	Au	1100 °C	1100 °C
A. Gomez-Martinez *et al.*, 2016[17e]	SiO from Si + residue O_2	Au (on Si substrate) or Cu foil	900 °C	900 °C
Z. D. Xiao *et al.*, 2006[19a]	Si substrate	Sn from SnO_2+C	1150 °C	500 °C
R. B. Wu *et al.*, 2007[19b]	Si powders	Fe	1500 °C	1500 °C
This Work	Si dissolving and releasing by Te species (from ZnTe +H_2)	Au	850 °C	758 – 565 °C

4 Conclusions

In summary, the SiO_x nanostructures discovered in the ZnTe growth was induced by the reaction intermediates, Te-based species. Growth mechanism study and analysis have revealed the different roles of the Te species and Au catalyst in the SiO_x nanostructure growth. The Te species dissolve the Si substrate by forming eutectic and then release Si vapor through subsequent evaporation. In the meanwhile, the Au catalysts accommodate the Si vapor to promote the growth. With the unique core-shell Au-Si catalyst structures, amorphous SiO_x nanostructures can form at different growth temperatures with various morphologies, including jellyfish-like nanowires, thick nanowires, nanorods, and nanospheres. This result indicates the importance of composition and phase control in the growth of compound nanostructures. Complicated intermediates might introduce unexpected compositions and even different phases into the deposition. This study also provides a new method for SiO_x nanostructures with low growth temperature and low cost with using expensive and hazardous precursors. The new growth mode could be further developed into a low-cost high-efficiency growth of 1D nanostructures of other materials.

Conflicts of interest

The authors declare no competing financial interest.

Acknowledgements

This work was supported by National Science Foundation (NSF) under grant DMR-1006547, and the start-up fund from the Department of Mechanical Engineering and Engineering Science (MEES) and Charlotte Research Institute at the University of North Carolina at Charlotte (UNC Charlotte), and the faculty research grant from UNC Charlotte. The authors appreciate the Department of MEES and the Center for Optoelectronics and Optical Communications at UNC Charlotte for the supports of multiuser facilities. T. S. thanks for the financial support from the

NSF DMR-1006547 and the teaching assistantship from the Optical Science and Engineering Program at UNC Charlotte. J. J. H. and E. O. thank the Research Experience for Undergraduate (REU) supports from the NSF DMR-1006547 and the MEES Summer REU program.

Notes and references

[a.] Department of Mechanical Engineering and Engineering Science, The University of North Carolina at Charlotte, 9201 University City Boulevard, Charlotte NC 28223

[b.] Department of Physics and Optical Science, and Optical Science and Engineering Program, The University of North Carolina at Charlotte, 9201 University City Boulevard, Charlotte NC 28223

[*.] Corresponding Author; Email: hzhang3@uncc.edu

1. Y. N. Xia, P. D. Yang, Y. G. Sun, Y. Y. Wu, B. Mayers, B. Gates, Y. D. Yin, F. Kim and Y. Q. Yan, *Adv. Mater.*, 2003, **15**, 353-389.
2. M. Law, J. Goldberger and P. D. Yang, *Ann. Rev. Mater. Res.*, 2004, **34**, 83-122.
3. Y. Y. Wu and P. D. Yang, *J. Am. Chem. Soc.*, 2001, **123**, 3165-3166.
4. (a) H. J. Fan, P. Werner and M. Zacharias, *Small*, 2006, **2**, 700-717; (b) Jessica L. Lensch-Falk, Eric R. Hemesath, Daniel E. Perea and Lincoln J. Lauhon, *J. Mater. Chem.*, 2009, **19**, 849-857.
5. (a) H. Chandrasekaran, G. U. Sumanasekara and M. K. Sunkara, *J. Phys. Chem. B*, 2006, **110**, 18351-18357; (b) Zheng Wei Pan, Zu Rong Dai, Chris Ma and Zhong L. Wang, *J. Am. Chem. Soc.*, 2002, **124**, 1817-1822.
6. Z. W. Pan, S. Dai, C. M. Rouleau and D. H. Lowndes, *Angew. Chem.-Int. Edit.*, 2005, **44**, 274-278.
7. (a) Junli Wang, Kangmin Chen, Ming Gong, Bin Xu and Qing Yang, *Nano Lett.*, 2013; (b) Tao Sheng, Baobao Cao, Yong Zhang and Haitao Zhang, *CrystEngComm*, 2015, **17**, 1139-1150.
8. (a) H. T. Zhang, T. T. Xu, M. Z. Tang, T. H. Her and S. Y. Li, *J. Vac. Sci. Technol. B*, 2010, **28**, 310-315; (b) Tao Sheng, Padmanabha P. Chavvakula, Baobao Cao, Naili Yue, Yong Zhang and Haitao Zhang, *J. Cryst. Growth*, 2014, **395**, 61-67; (c) Tao Sheng and Haitao Zhang, in *High-capacity Optical Networks and Emerging/Enabling Technologies (HONET), 2014 11th Annual*, 2014, pp. 219-222.
9. Muhammad Iqbal Bakti Utama, Maria de la Mata, Qing Zhang, Cesar Magen, Jordi Arbiol and Qihua Xiong, *Cryst. Growth Des.*, 2013, **13**, 2590-2596.

10. (a) Y. L. Cao, Y. B. Tang, Y. Liu, Z. T. Liu, L. B. Luo, Z. B. He, J. S. Jie, Roy Vellaisamy, W. J. Zhang, C. S. Lee and S. T. Lee, *Nanotechnology*, 2009, **20**, 455702; (b) S. Y. Li, Y. Jiang, D. Wu, L. Wang, H. H. Zhong, B. Wu, X. Z. Lan, Y. Q. Yu, Z. B. Wang and J. S. Jie, *J. Phys. Chem. C*, 2010, **114**, 7980-7985.
11. David R. Lide, ed., *CRC Handbook of Chemistry and Physics*, CRC Press, Boca Raton, Florida, 2003.
12. National Physical Laboratory, Kaye and Laby Tables of Physical and Chemical Constants, http://www.kayelaby.npl.co.uk/, Accessed May, 2018, 2018.
13. H. Okamoto and T. B. Massalski, *Bull. Alloy Phase Diagr.*, 1983, **4**, 190-198.
14. B. Legendre, C. Souleau, C. Hancheng and N. Rodier, *J. Chem. Res. (S)*, 1978, 168-169.
15. C. B. Alcock, V. P. Itkin and M. K. Horrigan, *Can. Metall. Quart.*, 1984, **23**, 309-313.
16. Z. W. Pan, S. Dai, D. B. Beach and D. H. Lowndes, *Nano Lett.*, 2003, **3**, 1279-1284.
17. (a) C. L. Pang, H. Cui and C. X. Wang, *Crystengcomm*, 2011, **13**, 4082-4085; (b) M. N. Banis, Y. Zhang, R. Y. Li, X. L. Sun, X. X. Jiang and D. Nikanpour, *Particuology*, 2011, **9**, 458-464; (c) J. Y. Qu, Z. B. Zhao, X. Z. Wang, J. S. Qiu and Y. Gogotsi, *Mater Express*, 2012, **2**, 157-163; (d) R. G. Elliman, T. H. Kim, A. Shalav and N. H. Fletcher, *J. Phys. Chem. C*, 2012, **116**, 3329-3333; (e) A. Gomez-Martinez, F. Márquez and C. Morant, *Appl. Surf. Sci.*, 2016, **387**, 1072-1079.
18. (a) A. Gomez-Martinez, F. Marquez and C. Morant, *Appl. Surf. Sci.*, 2015, **345**, 44-48; (b) A. Shalav, T. Kim and R. G. Elliman, *IEEE J. Sel. Top. Quantum Electron*, 2011, **17**, 785-793.
19. (a) Z. D. Xiao, L. D. Zhang, G. W. Meng, X. K. Tian, H. B. Zeng and M. Fang, *J. Phys. Chem. B*, 2006, **110**, 15724-15728; (b) R. B. Wu, B. S. Li, M. X. Gao, Q. M. Zhu, Y. Pan, G. Y. Yang and J. J. Chen, *Appl. Phys. Lett.*, 2007, **91**.

Table of contents entry

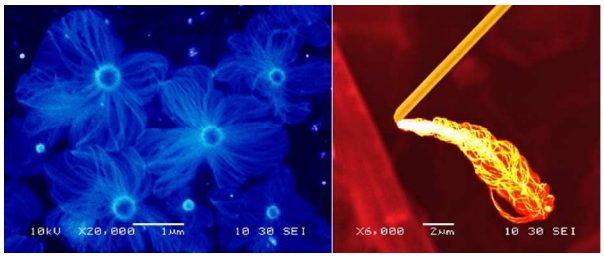

Jellyfish-like SiO_x nanowires were formed in a reaction intermediates induced vapor-liquid-solid process, which provides a new method for nanowire growth.